Inactivation of GalU leads the cell wall-associated polysaccharide defect to reduce the susceptibility to bacteriolytic agents in *Enterococcus faecalis*.

Jun Kurushima[1], Haruyoshi Tomita[1,2,#]

[1]Department of Bacteriology, Gunma University Graduate School of Medicine, 3-39-22, Showa-machi, Maebashi-shi, Gunma 371-8511, Japan

[2]Laboratory of Bacterial Drug Resistance, Gunma University Graduate School of Medicine, 3-39-22, Showa-machi, Maebashi-shi, Gunma 371-8511, Japan

[#]Corresponding author: Haruyoshi Tomita

E-mail: tomitaha@gunma-u.ac.jp

Phone: +81-27-220-7990. Fax: +81-27-220-7996

Running title: Role of *galU* on bacteriolysis in *E. faecalis*.

Keywords: Enterococcus, polysaccharide, galactose, antibiotic resistance, bacteriocin, morphogenesis, UDP-glucose phosphorylase, imaging, beta-lactam, cell death

Abstract (216 words)

Enterococcal plasmid-encoded bacteriolysin Bac41 is a selective antimicrobial system that is considered to provide a competitive advantage to *Enterococcus faecalis* cells that carry the Bac41-coding plasmid. The Bac41 effector consists of the secreted proteins $BacL_1$ and BacA, which attack the cell wall of the target *E. faecalis* cell to induce bacteriolysis. Here, we demonstrated that *galU*, which encodes UTP-glucose-1-phosphate uridylyltransferase, is involved in susceptibility to the Bac41 system in *E. faecalis*. Spontaneous mutants that developed resistance to the antimicrobial effects of $BacL_1$ and BacA were revealed to carry a truncation deletion of the C-terminal 288–298 a.a. region of the translated GalU protein. This truncation resulted in the depletion of UDP-glucose, leading to a failure to utilize galactose and produce the enterococcal polysaccharide antigen (EPA), which is expressed abundantly on the cell surface of *E. faecalis*. This cell surface composition defect that resulted from *galU* or EPA-specific genes caused an abnormal cell morphology, with impaired polarity during cell division and alterations of the limited localization of $BacL_1$. Interestingly, these mutants conferred reduced susceptibility to beta-lactams, despite their increased susceptibility to other bacteriostatic antimicrobial agents and chemical detergents. These data suggest that a complex mechanism of action underlies lytic killing, as exogenous bacteriolysis induced by lytic bacteriocins or beta-lactams requires an intact cell physiology

in *E. faecalis*.

Importance

Cell wall-associated polysaccharides of bacteria are involved in various physiological characteristics. Recent studies demonstrated that the cell wall-associated polysaccharide of *Enterococcus faecalis* is required for susceptibility to bactericidal antibiotic agents. Here, we demonstrated that a *galU* mutation resulted in resistance to the enterococcal lytic bacteriocin Bac41. The *galU* homologue is reported to be essential for biosynthesis of species-specific cell wall-associated polysaccharides in other Firmicutes. In *E. faecalis*, the *galU* mutant lost the *E. faecalis*-specific cell wall-associated polysaccharide EPA (enterococcal polysaccharide antigen). The mutant also displayed reduced susceptibility to antibacterial agents and an abnormal cell morphology. We firstly demonstrated that *galU* was essential for EPA biosynthesis in *E. faecalis,* and EPA production might underlie susceptibility to lytic bacteriocin and antibiotic agents by undefined mechanism.

Keywords

Enterococcus faecalis, bacteriocin, cell morphology, UDP-glucose phosphorylase,

55 beta-lactams

56

Introduction

Enterococcus faecalis is a Gram-positive opportunistic pathogen that is a causative agent of several infectious diseases, such as urinary infections, bacteremia, endocarditis, and others (1). This organism belongs to the lactic acid bacteria and is also a microbial resource that produces various bacteriocins (2). Bacteriocins are antimicrobial proteins or peptides that are produced by bacteria and are considered to play a role in bacterial competition within the microbial ecological environment (3). Gram-positive bacterial bacteriocins are classified according to their structures or synthetic pathways (4). Class I bacteriocins, which are referred to as lantibiotics, are heat-stable peptides that contain non-proteinogenic amino acids modified by post-translational modifications(5). Class II bacteriocins are also heat-stable peptides, but they are synthesized without any post-translational modification (6). In *E. faecalis*, beta-hemolysin/bacteriocin (cytolysin), which is the major virulence factor, and enterocin W belong to the class I bacteriocins (7–9). On the other hand, most enterococcal bacteriocins, including Bac21, Bac31, Bac32, Bac43, Bac51 and others, belong to the class II peptides(6, 8, 10–15) . Class III bacteriocins are proteinaceous heat-liable bacteriocins that differ from the class I or II peptides. Therefore, bacteriocins of this class are often referred to as bacteriolysins. Two enterococcal bacteriolysins, enterolysin A and Bac41, have been identified to date (16, 17).

The bacteriolysin Bac41 was originally found in the conjugative plasmid pYI14 of *E. faecalis* clinical strain YI14 and is widely distributed among clinical isolates including vancomycin resistant enterococci (VRE) (17–19). The activity of this bacteriocin is specific towards *E. faecalis* and not other *Enterococcus* or bacterial species (20). The genetic element of Bac41 consists of *bacL*$_1$, *bacL*$_2$, *bacA*, and *bacI*. BacL$_1$ and BacA are the effectors responsible for the antimicrobial activity of this bacteriocin against *E. faecalis*. BacL$_2$ is involved in the expression of antimicrobial activity as transcriptional positive regulator (17, 21). BacI is required for the self-protection of Bac41-producing *E. faecalis* cells from the antimicrobial activity of BacL$_1$ and BacA. Both the BacL$_1$ and BacA molecules contain conserved peptidoglycan hydrolase domains, suggesting that these molecules attack the target's cell wall (17). Endopeptidase activity against the *E. faecalis* cell wall has been detected experimentally in BacL$_1$ (22). However, the peptidoglycan degrading activity of BacA has not been detected, and the enzymatic function of this molecule remains unknown. BacL$_1$ binds specifically to the nascent cell wall or to cell division loci via its C-terminal SH3 repeat domain (20). The resulting cell growth inhibition protects against the binding of BacL$_1$ and markedly reduces susceptibility to bacterial killing by Bac41 effectors. It is important to note that the BacL$_1$ cell wall degradation process is essential but not sufficient to kill the bacteria; bacteriolysis requires the additional action of the undefined BacA.

In this paper, we isolated a spontaneous mutant of *E. faecalis* that exhibited resistance to the toxicity of $BacL_1$ and BacA to further understand the bacteriolytic mechanism of the Bac41 system. Genomic variant analysis showed that an intact *galU* gene was essential for susceptibility to $BacL_1$ and BacA. Furthermore, we demonstrated that *galU* is also essential for galactose fermentation and for the synthesis of the enterococcal polysaccharide antigen, which is required for maintaining the normal cell morphology and for susceptibility to antimicrobial agents.

Results

Inactivation of *galU* results in decreased susceptibility to Bac41. To identify the target *E. faecalis* cell factor(s) involved in Bac41-mediated bacterial killing, spontaneous mutants that are resistant to the Bac41 effectors $BacL_1$ and BacA were obtained. We carried out a soft-agar bacteriocin experiment in which the susceptible bacterial strain *E. faecalis* OG1S was inoculated into and grown in THB agar (0.75%), and a mixture of recombinant $BacL_1$ and BacA proteins (25 ng of each protein) was spotted onto the *E. faecalis*-containing THB agar. After incubation at 37 °C overnight, a clear growth inhibition zone was formed in the area where the recombinant proteins had been spotted (22). Notably, additional incubation resulted in the occurrence of small colonies within the growth inhibitory zone. These colonies were considered to be spontaneously resistant mutants, so we isolated these colonies as candidates that may carry a genetic mutation related to bacterial killing by Bac41. To identify the genetic mutation that caused this spontaneous Bac41 resistance, we performed whole-genome sequencing and a variant analysis of the mutant strains. The contigs from the genome sequence of the parent strain *E. faecalis* OG1S and the isogenic mutant were obtained by next generation sequencing and were mapped onto the reference strain *E. faecalis* OG1RF (accession No. NC_017316). One of these spontaneous mutants, sr #4, carried the point mutation C862T within the *galU* (annotated as *cap4C* in the OG1RF genomic information)

coding sequence (Fig. 1A). The wild-type *galU* gene consists of 897-bp, and its translated product GalU is 298 a.a. in length. The mutation found in sr #4 was a nonsense mutation and resulted in the truncation of the GalU protein by a C-terminal deletion of 288–298 a.a. (Fig. 1B). Complementation via the introduction of the intact *galU* gene carried by the expression vector p*galU* restored the mutant strain's susceptibility to Bac41 activity to the level of the parent strain (Fig. 1C). In addition, a liquid phase bacteriolytic assay also demonstrated that the spontaneous mutant (referred to as *galU*$^{-}$ hereafter) could still grow in the presence of recombinant $BacL_1$ (r$BacL_1$) and BacA (rBacA), while the wild-type strain underwent considerable lysis (Fig. 1D). The complementation of the *galU* mutation via the expression of intact *galU in trans* (*galU*$^{-}$/p*galU*) but not the control vector (*galU*$^{-}$/Vec) restored the strain's susceptibility to bacteriolysis to the same degree as the wild-type strain. The viability of the *galU*$^{-}$ and *galU*$^{-}$/Vec strains exhibited a >100-fold increase in comparison to the WT and *galU*$^{-}$/p*galU* strains after treatment with r$BacL_1$ and rBacA (5 μg/ml each) for 4 h (Fig. 1E). Therefore, these results strongly demonstrated that the truncated mutation of the *galU* gene resulted in resistance to the antimicrobial activity of Bac41.

The enterococcal *galU* is essential for the fermentation of galactose and the production

of cell wall-associated polysaccharides.

The *galU* gene encodes UDP-glucose phosphorylase (UDPG::PP, EC: 2.7.7.9), which generates UDP-glucose from a UTP molecule and glucose-1-phosphate (23). The homologues of this gene are universally conserved not only in prokaryotes but also in eukaryotes (24). It has been reported extensively that among both Gram-positive and Gram-negative bacteria, this enzymatic activity of GalU is essential for the carbohydrate metabolism that is involved in multiple bacterial physiological pathways; however, the precise role of GalU in *E. faecalis* remains undefined. UDP-glucose, which is the product of GalU, is utilized for galactose fermentation via the Leloir pathway in lactic acid bacteria (Fig. 2A) (25). We tested whether the strain that possesses an inactivated *galU* has the ability to undergo galactose fermentation (Fig. 2B). The wild-type strain and the complemented strain had the ability to ferment both glucose and galactose. In contrast, the *galU* mutant strain and the *galU*$^{-}$/Vec strain could utilize glucose but not galactose. In addition, the in-frame deletion mutants of *galU* that were constructed via site-directed mutagenesis also failed to utilize galactose in the two different lineages OG1RF and FA2-2 (Supplementary figure S1). These data clearly indicated that GalU produces UDP-glucose in *E. faecalis* and in other species and also suggested that the C-terminal truncation of GalU in the *galU*$^{-}$ strain resulted in the complete loss of its UDP-glucose phosphorylase (UDPG::PP) activity.

In addition to its role in galactose fermentation, GalU and its product, UDP-glucose, are essential for the biosynthesis of bacterial glycopolymers, such as LPS, teichoic acid and capsular polysaccharide, which are important structural components that determine the properties of the bacterial cell surface (26). For example, in *S. pneumoniae,* which has more than 90 capsular variants, GalU is essential for the biosynthesis of various types of capsular polysaccharide (Mollerach et al., 1998). The cell surface polysaccharide profiles of *E. faecalis* strains were previously demonstrated (27, 28) . To investigate the effect of the *galU* mutation on capsular polysaccharide synthesis in enterococci, cell wall-associated polysaccharides were prepared from the *E. faecalis* WT, *galU*$^-$, *galU*$^-$/Vec and *galU*$^-$/p*galU* strains and subjected to polyacrylamide gel electrophoresis analysis, followed by visualization with cationic staining (Fig. 2C). The most abundant band, which corresponds to the enterococcal polysaccharide antigen (EPA), was observed in the wild-type OG1S and *galU*$^-$/p*galU* strains. In contrast, the EPA had completely disappeared in the *galU*$^-$ and *galU*$^-$ /vector strains. This result strongly suggested that the *galU* gene is essential for EPA production in *E. faecalis*.

Previous studies identified the specific EPA biosynthesis gene cluster *epaA–R* (27, 29, 30). Several *epa* gene mutants with altered EPA composition, such as mutants of *epaA, B, E, M, N, I, X* or *O,* displayed a pleiotropic phenotype that included abnormal cell

171 morphology, defective biofilm formation, and increased susceptibility to antimicrobial agents
172 and phages, as well as other phenotypes (30, 31). We investigated the effect of *galU*
173 inactivation on cell morphology. *E. faecalis* is an ovococcal bacterium with an ellipsoid-cell
174 shape, and its size is approximately 2 μm by 1 μm. Observation under a scanning electron
175 microscope revealed that the *galU*$^-$ strain showed an abnormal cell morphology with a
176 rounded cell shape and a slightly larger size (~2 μm) (Fig. 3A). Fluorescent imaging using
177 DAPI, which is a fluorescence probe for DNA, revealed that abnormal multinucleated cells
178 were present in the *galU*$^-$ population (Fig. 3B). The complemented strain *galU*$^-$/p*galU* but
179 not the control vector *galU*$^-$/Vec showed the same morphological phenotype as the wild-type
180 strain. These observations suggested that the truncation of the *galU* gene leads to a marked
181 morphological defect.
182
183 **The loss of cell wall-associated EPA does not block targeting and cell wall degrading of**
184 **BacL$_1$ to the cell wall.**
185 We previously reported that the peptidoglycan degradation activity of BacL$_1$ is not
186 sufficient but still essential for Bac41-mediated bacterial killing (22). We examined whether
187 the observed resistance to Bac41 activity in the *galU*$^-$ mutant results from decreased
188 susceptibility of the cell wall to BacL$_1$. Cell wall fractions prepared from the wild-type OG1S

189 strain and the *galU*$^-$, *galU*$^-$/Vec or *galU*$^-$/p*galU* strains were treated with recombinant $BacL_1$,
190 followed by incubation at 37 °C (Fig. 4A). The cell walls from the parent strain and the
191 complemented strain were degraded to 52.8% and 51.9% of the initial amount after 6 hours
192 of incubation, respectively. In contrast, the *galU*$^-$- and *galU*$^-$/Vec-derived cell walls were also
193 degraded to 70.6% and 68.5%, respectively, by $BacL_1$, although degradation rates were
194 slightly attenuated compared to those of the parent strain and the complemented strain. In
195 addition, the cell walls of *galU*$^-$ and *galU*$^-$/Vec also displayed reduced susceptibility to
196 mutanolysin, which is a peptidoglycan hydrolase but has no capacity to induce definite
197 bacteriolysis (Supplementary figure S2) (22). These observations suggested the possibility
198 that cell wall of *galU* mutant is still susceptible to peptidoglycan hydrolase activity of $BacL_1$.
199 The binding of $BacL_1$ via its C-terminal SH3 repeat domain, which is located in 329–380 a.a.,
200 is limited to the cell division loci of the target cell wall and is essential for the peptidase
201 activity of $BacL_1$ (22). To investigate whether the binding affinity of $BacL_1$ for the *galU*$^-$ cell
202 wall was involved in attenuated susceptibility to degradation by $BacL_1$, fluorescence-labeled
203 recombinant $BacL_1$ was incubated with *E. faecalis* cells and its localization was analyzed by
204 fluorescent microscopy. In the parent strain and the complemented strain, $BacL_1$ binding was
205 limited to division loci, as reported previously (Fig. 4B, Supplementary figure S3A) (20). In
206 *galU*$^-$ mutant, $BacL_1$ strongly bound to over the cells surface even more diffusely and was

207 less limited to specific target loci, showing that the affinity of $BacL_1$ for the cell wall the
208 *galU*$^-$ strain appeared to be even more increased compared to those of wild type. These
209 observations suggested that attenuated susceptibility to $BacL_1$ degradation is not likely cause
210 of the development of Bac41 resistance in the *galU* mutant, even though the overall cell
211 surface affinity for $BacL_1$ was altered in the *galU*$^-$ *mutant*.

212 To investigate whether the phenotypes of the *galU*$^-$ mutant resulted specifically
213 from the loss of cell wall-associated polysaccharides, we constructed a deletion mutant of
214 *epaB*, which is involved in the major EPA biosynthesis pathway (Fig. 5A) (31). The
215 inactivation of *epaB* is suggested to result in an altered EPA structure and composition and
216 reduced cell envelope integrity. The *epaB* mutant (Δ*epaB*) no longer produces EPA (30, 32),
217 meanwhile it displayed normal galactose fermentation as like wild type (Supplementary
218 figure S4). Notably, the Δ*epaB* clearly represented resistance to Bac41 as *galU*$^-$ mutant (Fig
219 5B and C), suggesting that Bac41 resistance in *galU*$^-$ mutant is mostly due to inability of EPA
220 production.

221 To test whether $BacL_1$ degradation susceptibility of cell wall lacking EPA, cell wall
222 purified from the Δ*epaB* mutant was subjected to cell wall degradation assay (Supplementary
223 figure S5). $BacL_1$ was able to degrade cell wall of all tested strains including the Δ*epaB*,
224 Δ*galU* (*galU* in-frame deletion) and their derivatives with plasmids for complementation as

well as wild-type strain. In addition, $BacL_1$ could bind to cell surface of the Δ*epaB* mutant as wild type (Fig. S3B). In order to characterize localization of $BacL_1$ binding on each strain in detail, we observed relative subcellular-localization of fluorescein-labeled SH3-repeat of $BacL_1$ ($BacL_1$_SH3), which expresses strong and stable fluorescence signal compared to full-length $BacL_1$ protein (20), on wild type, the Δ*galU* and the Δ*epaB* mutants (Fig. 5D). On demograph based on microscope image, $BacL_1$_SH3 bound around division site of Δ*galU* and Δ*epaB* eually to wild type as previously reported (20). It is noted that $BacL_1$_SH3 localization in the Δ*galU* mutant was even stronger and more dispersed on the cell surface comapred to wild type. These observations are in line with our previously mentioned hypothesis that alternation of cell wall integrity does not affect $BacL_1$ targeting for endopeptidase activity and does not underlie resistant phenotype of these mutant against Bac41-indused cell lysis.

The *galU* inactivation and loss of EPA reduce susceptibility to beta-lactams.

It has been suggested that EPA deficiency results in reduced cell surface integrity and consequently leads to increased susceptibility to antimicrobial agents or several environmental stress (31, 33, 34). To test this phenotype in the *galU*$^-$ strain, we evaluated susceptibility to antibiotics in the OG1S derivatives (Table 2). Consistent with previous

reports, bacteriostatic antibiotics (vancomycin and gentamycin) and detergent (sodium dodecyl sulfate (SDS)) were more effective against the *galU*$^{-}$ and *galU*$^{-}$/Vec strains than the wild-type and complemented strains. In contrast, the MICs of beta-lactams (ampicillin and penicillin G) for the *galU*$^{-}$ strain were 4 mg/L and 2 mg/L, respectively, indicating reduced susceptibility in comparison to the parent strain. As already shown by Singh and Murray (35), the Δ*epaB* strain also displayed higher MICs and reduced susceptibility for beta-lactams than its parent (Table 2, Fig. 5C). The viability of the *galU*$^{-}$ mutant after treatment with ampicillin (ABPC; 4 mg/L) for 4 h was increased approximately 10-fold in comparison to the wild-type strain (Fig. 6A). In microscopic experiments, the wild-type strain displayed morphological changes, with an elongated or rhomboid shape after 60 min of treatment with ABPC (4 mg/L), and most cells exhibited drastic cell disruption between 90 and 180 min after the treatment (Fig. 6B). On the other hand, the *galU*$^{-}$ strain displayed a milder phenotype, with a swollen shape, showing a response distinct from that of the wild-type strain (Fig. 6B). In addition, only a few disrupted *galU*$^{-}$ cells were observed, even 180 min after treatment with AMP. To distinguish between a bacteriolytic effect and a growth inhibition (bacteriostatic) effect of AMP, the turbidity of bacterial broth cultures was monitored in the presence and absence of ABPC (4 mg/L) (Fig. 6C). In the wild-type strain, the turbidity was increased after 60 min of incubation, in the presence of ABPC and in the mock control. However, after 90 min, a drastic

261 reduction of turbidity was detected, and the turbidity was eventually lower than the initial
262 turbidity. In contrast, after exposure to AMP, the *galU*$^{-}$ strain continued to grow constantly
263 without reduced turbidity, although its growth rate was slower than that of the untreated
264 culture. These results were consistent with the microscopic observations, in that the *galU*$^{-}$
265 mutant could be susceptible to the bacteriostatic effect of ABPC but not to the bacteriolytic
266 effect. Furthermore, fluorescently detection assay for cell lysis by Ethidium homodimer
267 (EthD) clearly showed that ABPC treatment increased dead cell population in wild type (Fig.
268 6D and E). On the other hand, the Δ*galU* and Δ*epaB* mutants did not show significant
269 increases of dead cell population compared to un-treatment control. Also, cell elongation
270 effect of ABPC is relatively less in the Δ*galU* and the Δ*epaB* mutants while ABPC treatment
271 resulted in the significant elongation of cell length in wild type (Fig. 6F). Altogether, these
272 data suggested that unlike other drugs and detergents, the bacteriolytic action of beta-lactams
273 requires an intact cell surface composition constructed by the *galU* or *epa* genes.

Discussion

The function of the *E. faecalis* GalU C-terminus

Here, we demonstrated that a spontaneous Bac41-resistant isolate carried a truncation mutation in the *galU* gene, with the deletion of 11 C-terminal residues (Fig. 1). Like related species, the GalU of *E. faecalis* contains a conserved nucleotide transferase domain at 5–257 a.a (Supplementary figure S6 and S7). However, the resistant mutant has a truncation deletion of 288–298 a.a., which does not correspond to the conserved domain. Despite this anomaly, this partial truncation leads to the inactivation of the protein's UDP-glucose phosphorylase activity (Fig. 2 and Supplementary figure S1). Structural studies of GalU homologues from several bacterial species revealed that their C-terminal domains entangled each other to form homo-dimers (36, 37). Thus, it is possible that the deletion of just 11 amino acids from the C-terminal moiety might impair this dimerization, resulting in a conformational defect that affects GalU enzymatic activity.

The role of *galU* in cell wall polysaccharide production in *E. faecalis* strains

The *gpsA-galU* locus is conserved among *Enterococcus* and *Streptococcus* species, although its chromosomal location and flanking genetic context are unrelated (Supplementary figure S7). This locus has been best studied in *Streptococcus pneumoniae*,

292 which is a bacterial pathogen that causes pneumonia in humans (38). The surface capsular
293 polysaccharide (CPS) of *S. pneumoniae* is a major virulence factor and the target for
294 vaccination. More than 90 CPS types that have been defined in *S. pneumoniae* are
295 synthesized from the corresponding specific *cps* locus, which is located between *pbp2X* and
296 *pbp1A* (39). Although the *cps* genes are variable and specific for each of the 90 capsule types,
297 *gpsA-galU* is highly conserved in a location that is distant from *cps* and is essential for the
298 biosynthesis of every capsule type (40). Thus, *gpsA-galU* is suggested to play a critical role
299 in the highly conserved universal pathway for cell surface-associated polysaccharides in
300 various lactic acid bacterial species (41, 42). For *E. faecalis*, four serotypes (A, B, C and D)
301 have been identified (43). These serotypes are defined by variants of two cell surface
302 components: CPS and EPA (44). The CPS is serotype-specific and is represented only in
303 serotypes C and D but not in serotypes A and B (28). Conversely, EPA is represented in every
304 *E. faecalis* strain with any serotype. OG1 strains belong to the serotype B lineage that
305 possesses only EPA. Meanwhile, the serotype C strains, such as FA2-2 and V583, produce
306 both EPA and CPS (43, 44). Teng *et al*. identified the EPA-synthesizing *epa* gene cluster
307 (locus tag 11715–11738), which is distant from the *gpsA-galU* locus (locus tag 11457 and
308 11458), on the OG1RF chromosome (29, 31). Recent study by Guerardel *et al*. defined
309 structure of EPA and it consists of several sugars, including glucose, galactose, rhamnose,

and ribitol (27). According to previous studies of capsular polysaccharide synthesis, those sugars are utilized to construct the cell wall glycopolymer through uridyl-nucleotide intermediates, such as UDP-glucose, which is produced by GalU. The data showing that the inactivation of the *galU* gene caused the abolishment of EPA (Fig. 2C) demonstrated the involvement of the *gpsA-galU* locus in the universal biosynthetic pathway for cell surface polysaccharide species in *E. faecalis*, which is similar to available reports for *S. pneumoniae*. The deletion of *galU* resulted in the complete loss of cell wall-associated polysaccharides in the serotype C *E. faecalis* FA2-2 (Supplementary figure S8), suggesting that GalU also plays a role in CPS production. This study is the first report to describe the function of *galU* in the biosynthesis of cell wall-associated polysaccharides in *E. faecalis*.

Deduced model of *galU*-dependent susceptibility to lytic agents

A previous study revealed that the inactivation of *galU* decreases cellular robustness against several stresses, such as antibiotics and H_2O_2 (45). Here we confirmed that the *galU*$^-$ strain displayed lower MICs for gentamicin, daptomycin and SDS in comparison to the parent strain (Table 2). However, we focused on the opposite phenotype that the inactivation of *galU* conferred resistance to the lytic bacteriocin Bac41 ($BacL_1$ and BacA) and beta-lactams (Fig. 1, Fig. 6 and Table 2). In comparison with the wild-type strain,

328 the *galU*$^{-}$ strain produced a cell wall with slightly reduced susceptibility to $BacL_1$ degradation
329 (Fig. 4A). The contribution of this phenotype to resistance should be partial, and this process
330 did not appear to be the fundamental mechanism by which the bacteriolytic activity of Bac41
331 is triggered by the undefined action of BacA following peptidoglycan degradation by $BacL_1$
332 (20). UDP-glucose is essential for the biosynthesis of not only cell surface polysaccharides
333 but also other cell wall-associated components, such as teichoic acid. The Δ*epaB* mutant that
334 displayed a specific EPA defect conferred Bac41 resistance, as observed for the *galU*$^{-}$ mutant
335 (Fig. 5C). However, we cannot conclude that EPA contributed exclusively or directly to
336 susceptibility to Bac41 because both mutants displayed the characteristic phenotype of
337 abnormal cell morphology (Fig. 3 and Fig. 5) (30), suggesting that this drastic phenotype is
338 caused by the loss of envelope integrity that results from the depletion of cell wall-associated
339 polysaccharides (31). It is worth noting that the morphological defects observed in the *galU*
340 and *epaB* mutants were not identical, which implies that other UDP-glucose-derived
341 components might affect the phenotype of the *galU* mutant. In *Bacillus subtilis*, which is a
342 model organism for Fermicutes, GtaB (a GalU homologue) is indispensable for cell
343 morphology. The GtaB-deficient mutant exhibits a dislocation of FtsZ, which is a conserved
344 protein that determines the contracting (separating) site during binary cell division, and the
345 mutant consequently exhibits impaired cell division with an abnormal cell shape(46). As

346 shown in Fig. 4, the *galU*$^{-}$ mutant gave rise to a dispersed localization of $BacL_1$, which binds
347 specifically to the nascent cell wall and displays a limited localization at the mid-cell in the
348 wild-type strain (20). Since the cell division machinery complex performs dual functions
349 (synthesize and degrade peptidoglycan), the failure to properly control this machinery,
350 especially the inhibition of penicillin binding proteins (PBPs), leads to lethal effects on
351 bacterial cells. The potential intrinsic lethality of the cell division machinery has been
352 suggested to underlie beta-lactam-induced bacteriolysis (47). Therefore, it is possible that
353 the deactivated cell division machinery in the *galU*$^{-}$ and Δ*epaB* mutants reduces the intrinsic
354 lethality of the cell division machinery, resulting in resistance to Bac41 or beta-lactams.
355 Collectively, this study provides insights into the intrinsic factors involved in the extrinsic
356 bacteriolysis mechanism in *E. faecalis*, but further investigation is required to understand the
357 precise mechanism that underlies these effects.
358

359 **Experimental procedures**

360 **Bacterial strains, plasmids and antimicrobial agents.**

361 The bacterial strains and the plasmids used in this study are shown in Table 1.
362 *Enterococcal* strains were routinely grown in Todd-Hewitt broth (THB) (Difco, Detroit, MI)
363 at 37 °C (48), unless stated otherwise. *Escherichia coli* strains were grown in Luria-Bertani
364 (LB) (Difco) medium at 37 °C. The antibiotic concentrations used to select *E. coli* were 100
365 mg/L of ampicillin (AMP), 30 mg/L of chloramphenicol and 500 mg/L of erythromycin. The
366 concentrations used for the routine selection of *E. faecalis* harboring pMGS100 or
367 pMSP3535 derivatives were 20 mg/L of chloramphenicol or 10 mg/L of erythromycin,
368 respectively. Nisin was added at a concentration of 25 mg/L for the cultivation of the *E.*
369 *faecalis* strain harboring pMSP3535. All antibiotics were obtained from Sigma Co. (St. Louis,
370 MO).

371

372 **Soft-agar bacteriocin experiment.**

373 The soft-agar assay for bacteriocin activity was performed as described previously
374 (7). Briefly, 1 µL of recombinant protein solution (25 ng/µl) was inoculated into THB soft-
375 agar (0.75%) containing the indicator strain and was then incubated at 37 °C for 24 h. The
376 formation of an inhibitory zone was evaluated as sign of bacteriocinogenic activity of the test

377 strain. The histidine-tagged recombinant proteins of $BacL_1$ and BacA were prepared by the
378 Ni-nitrilotriacetic acid (Ni-NTA) system (Invitorogen, Carlsbad, CA) as previously described
379 (22).
380
381 **Next generation sequencing and variant analysis.**
382 Genomic DNA (gDNA) was extracted from *E. faecalis* OG1S and its isogenic
383 spontaneous mutant using an Isoplant DNA isolation kit (Nippon gene, Tokyo, Japan)
384 according to the manufacturer's instructions, and submitted to Otogenetics Corporation
385 (Norcross, GA USA) for exome capture and sequencing. Briefly, gDNA was subjected to
386 agarose gel electrophoresis and OD ratio tests to confirm the purity and concentration of the
387 DNA prior to Bioruptor (Diagenode, Inc., Denville, NJ USA) fragmentation. Fragmented
388 gDNAs were tested for size distribution and concentration using an Agilent Bioanalyzer 2100
389 or Tapestation 2200 and Nanodrop. Illumina libraries were made from qualified fragmented
390 gDNA using SPRIworks HT Reagent Kit (Beckman Coulter, Inc. Indianapolis, IN USA,
391 catalog# B06938) or NEBNext reagents (New England Biolabs, Ipswich, MA USA, catalog#
392 E6040) and the resulting libraries were then sequenced on an Illumina HiSeq2000/2500
393 which generated paired-end reads of 100 nucleotides (nt). Data was analyzed for data quality
394 using FASTQC (Babraham Institute, Cambridge, UK).

Construction of expression plasmids.

To complement the *galU* defect in the *galU*$^-$ strain, a *galU* expression plasmid designated as p*galU* was constructed as described below. A 927-bp fragment containing the full-length *galU* gene (897-bp) and an additional sequence at both ends (15-bp each) was amplified by PCR with the primers F-*galU*-pMGS and R-*galU*-pMGS, using *E. faecalis* OG1S genomic DNA as the template. Using In-fusion HD cloning (Clontech, Mountain View, CA), the resulting fragment was cloned into pMGS100 (49), which was linearized by digestion with *Nde*I and *Xho*I. The resulting plasmid was designated p*galU*. To complement the *epaB* defect, an *epaB* expression plasmid designated as p*epaB* was constructed as described below. An 819-bp fragment containing the full-length *epaB* gene (OG1RF_11737, 789-bp) and an additional sequence at both ends (15-bp each) was amplified by PCR with the primers F-*epaB*-pMSP3535 and R-*epaB*-pMSP3535, using *E. faecalis* OG1RF genomic DNA as the template. Using In-fusion HD cloning (Clontech, Mountain View, CA), the resulting fragment was cloned into pMSP3535 (50), which was linearized by digestion with *Bam*HI. The resulting plasmid was designated p*epaB*.

Site-directed in-frame deletion of *galU*.

Site-directed mutagenesis was carried out as described previously by Kristich *et al* (51). The 1-kbp flanking DNA fragments of the upstream or downstream regions of *galU* (OG1RF previously annotated *cap4C*) were amplified by PCR with the primers F-*galU*-del-up and R-*galU*-del-up or F-*galU*-del-dwn and R-*galU*-del-dwn, respectively, using *Enterococcus faecalis* OG1RF genomic DNA as the template. The resulting fragments were fused via overlapping PCR with the primers F-*galU*-del-up and R-*galU*-del-dwn, and the resulting 2-kb fragment was digested with *Eco*RI and cloned into pCJK47 at its *Eco*RI site to obtain pCJK47::Δ*galU*. The pCJK47::Δ*galU* plasmid was introduced into *E. faecalis* CK111 and was then transferred into *E. faecalis* OG1RF and FA2-2. The integrants of OG1RF and FA2-2 in which pCJK47::Δ*galU* was integrated into the chromosome via primary crossing over were isolated through erythromycin selection. Cultivation without the drug allowed crossing over to facilitate the drop out of pCJK47 derivatives. The isolated candidates were screened by PCR with primers that were set outside of the region used for cloning into pCJK47. The site-directed deletion of the *epaB* gene was also carried out as described above, except pCJK47::Δ*epaB* was constructed using specific primer pairs (F-*epaB*-del-up and R-*epaB*-del-up or F-*epaB*-del-dwn and R-*epaB*-del-dwn) for the upstream region or the downstream region, respectively. Both the Δ*galU* and Δ*epaB* mutants carry the initial 30 nt from the start codon and the terminal 30 nt, including the stop codon, without a

frame-shift (N-terminal 10 a.a. and C-terminal 9 a.a.). The mutant genes encode the 19 a.a. fusion proteins with N-terminal 10 a.a. and C-terminal 9 a.a. regions.

Scanning electron microscopy.

A 200 µL overnight culture of bacteria was diluted 5-fold with 800 µL of fresh THB, and transferred onto a coverslip grass (Iwanami) in 24-well plate following incubation at 37 °C for 2 h (Iwanami). The coverslip was rinsed with 1 mL of 0.1M cacodylate buffer (pH 7.4). The bacteria on the coverslip were fixed with 1 mL of 1st fixation buffer [2% glutaraldehyde, 4% sucrose, 0.15% alcian blue, 0.1M cacodylate buffer (pH 7.4)] for 2 h at room temperature (RT). After primary fixation, the coverslip was washed three times with 0.1M cacodylate buffer (pH 7.4). An additional fixation was carried out with 1 mL of 2nd fixation buffer [0.5% OsO_4, 0.1M cacodylate buffer (pH 7.4)] for 2 h at RT. The coverslip was washed with 0.1M cacodylate buffer (pH 7.4). The sample was dehydrated using an ascending ethanol series [50% (1 min), 70% (2 min), 80% (3 min), and 100% (5 min ×2)] and was air-dried. Osmium coating was carried out at 5–6 mA, for 20 sec using an Osmium coater (Neoc-ST, Meiwafosis CO., LTD, Tokyo, Japan). The sample was observed in the Scanning electron microscopy (S-4100, Hitachi, Tokyo, Japan).

449 **Fluorescent microscopy.**

450 The red fluorescent dye-labeled recombinant protein of $BacL_1$ was prepared with
451 NH_2-reactive HiLyte Fluor 555 (Dojindo, Kumamoto, Japan) as previously described (20).
452 Bacteria diluted with fresh medium were mixed with fluorescent recombinant protein and
453 incubated at 37 °C for 1 h. The bacteria were collected by centrifugation at 5,800 g for 3 min
454 and then fixed with 4% paraformaldehyde at room temperature (RT) for 15 min. The bacteria
455 were rinsed and resuspended with distilled water and mounted with Prolong gold antifade
456 reagent with 4', 6-di-amidino-2-phenylindole (DAPI; Invitrogen) on a glass slide. The
457 sample was analyzed by fluorescence microscopy (Axiovert 200; Carl Zeiss, Oberkochen,
458 Germany), and images were obtained with a DP71 camera (Olympus, Tokyo, Japan). For
459 detection of dead cells, ethidium homodimer (EthD, Molecular probe) was added in bacterial
460 culture at the final concentration of 2 μM and prepared for the microscopic analysis as
461 described above. Raw image data were processed using FIJI(52). Cell segmentation and
462 generation of fluorescence signal demograph were performed by Oufti(53). Statistical
463 analysis and graphical representation on imaging data acquired by Oufti was performed by
464 using R packages BactMAP(54) and ggplot2(55).
465

Preparation and degradation analysis of the cell wall fraction.

The bacterial culture was collected by centrifugation and rinsed with 1 M NaCl. The bacterial pellet was suspended in 4% SDS and heated at 95°C for 30 min. After rinsing with distilled water (DW) four times, unbroken cells were removed by centrifugation at 1,000 rpm for 1 min and the cell wall fraction in the supernatant was collected by centrifugation at 15,000 rpm for 10 min and was then treated with 0.5 mg/mL trypsin (0.1 M Tris-HCl [pH 6.8], 20 mM $CaCl_2$) at 37 °C for 16 h. The sample was further washed with DW four times and was resuspended in 10% trichloroacetic acid (TCA), followed by incubation at 4°C for 5 h, and then given four additional washes with DW. Finally, the cell wall fraction was resuspended in PBS. The cell wall degradation rate was quantified by measuring the optical density at 620 nm (OD_{620}) using a microplate reader (Thermo).

Preparation of cell surface polysaccharides.

Cell surface polysaccharides were prepared as described by Hancock and Gilmore (44). An overnight bacterial culture was inoculated with as a 1:100 dilution into 25 ml of THB containing with 1% glucose and grown at 37 °C for 5 h and then centrifuged to collect the cells (3,000 rpm, 10 min). The cells were washed with 2 ml of Tris-Sucrose solution [10 mM Tris (pH8.0), 25% sucrose]. The resulting cell pellets were resuspended in the Tris-

Sucrose solution containing lysozyme (1 mg/ml) and mutanolysin (10 U/ml), and incubated at 37 °C for 16 h. The suspension was then centrifuged (8,000 rpm, 3 min). The supernatant was collected into a new tube and was treated with RNase I (100 µg/ml) and DNase I (10 U/ml) at 37 °C for 4h. Pronase E was added (20 µg/ml) and the sample further incubated at 37 °C for 16 h. 500 µl of chloroform was added to the sample, which was then centrifuged (12,000, 10 min). The aqueous phase (~300 µl) was transferred into a new tube and 920 µl of ethanol added (final concentration, 75%) to precipitate the contents at -80°C for 30 min. The precipitate was pelleted by centrifugation (15,000 rpm, 10 min), air dried, and resuspended with 100 µl of DW into one tube. Approximately 2.5 µl of the resulting sample was subjected to 10% acrylamide gel electrophoresis buffered by TBE (10mM Tris, 10 mM borate, 2 mM EDTA). The separated carbohydrates were visualized with Stains-All (Sigma).

Fermentation test.

Fermentation of the respective sugar was examined as described before (40). Briefly, the *E. faecalis* strains were streaked on Heart infusion (HI, Difco) agar supplemented with 1% glucose or 1% galactose. Phenol red was added as a pH indicator at the final concentration of 25 ppm. After incubation overnight at 37 °C, fermentation was evaluated by the appearance of bacterial colonies and acidification of the agar medium.

502

503 **Antimicrobial susceptibility testing**

504 The MICs of the antibiotics were determined by the agar dilution method according
505 to CLSI recommendations [Clinical and Laboratory Standards Institute (http://clsi.org/)]. An
506 overnight culture of each strain grown in Mueller-Hinton broth (Nissui, Tokyo, Japan) was
507 diluted 100-fold with fresh broth. An inoculum of approximately $5x10^5$ cells was spotted
508 onto a series of Mueller-Hinton agar (Eiken, Tokyo, Japan) plates containing a range of
509 concentrations of the test drug. After incubation at 37 °C for 24 h, the number of colonies
510 that had grown on the plates was determined.

511

Acknowledgements

We thank Dr. Gary Dunny for providing the bacterial strains and the plasmids used to construct the mutants, Ms. Mari Arai and Ms. Satomi Tsuchihashi for providing technical assistance in this study, and Dr. Elizabeth Kamei for providing English proofreading of this manuscript.

Funding information

This work was supported by grants from the Japanese Ministry of Education, Culture, Sport, Science and Technology [Kiban (C) 18K07101, Grant-in-Aid for Young Scientists (B) 25870116, Gunma University Operation Grants] and the Japanese Ministry of Health, Labor and Welfare (the Research Program on Emerging and Re-emerging Infectious Diseases from Japan Agency for Medical Research and Development (AMED [20fk0108061h0503, 20wm0225008h0201]), H27-Shokuhin-Ippan-008).

References

1. Arias, C. A., and Murray, B. E. (2012) The rise of the Enterococcus: beyond vancomycin resistance. *Nature Reviews Microbiology*. **10**, 266–278

2. Nes, I. F., Diep, D. B., and Holo, H. (2007) Bacteriocin Diversity in Streptococcus and Enterococcus. *Journal of bacteriology*. **189**, 1189–1198

3. Nes, I. F., Clewell, D. B., Ike, Y., Shankar, N., and Diep, D. B. (2014) Enterococcal Bacteriocins and Antimicrobial Proteins that Contribute to Niche Control

4. Jack, R. W., Tagg, J. R., and Ray, B. (1995) Bacteriocins of gram-positive bacteria. *Microbiological reviews. Baltimore*. **59**, 171–200

5. Field, D., Hill, C., Cotter, P. D., and Ross, R. P. (2010) The dawning of a "Golden era" in lantibiotic bioengineering. *Molecular microbiology*. **78**, 1077–1087

6. Aymerich, T., Holo, H., Håvarstein, L. S., Hugas, M., Garriga, M., and Nes, I. F. (1996) Biochemical and genetic characterization of enterocin A from Enterococcus faecium, a new antilisterial bacteriocin in the pediocin family of bacteriocins. *Applied and Environmental Microbiology*. **62**, 1676–1682

7. Ike, Y., Clewell, D. B., Segarra, R. A., and Gilmore, M. S. (1990) Genetic analysis of the pAD1 hemolysin/bacteriocin determinant in Enterococcus faecalis: Tn917 insertional mutagenesis and cloning. *Journal of bacteriology*. **172**, 155–163

8. Sawa, N., Wilaipun, P., Kinoshita, S., Zendo, T., Leelawatcharamas, V., Nakayama, J., and Sonomoto, K. (2012) Isolation and characterization of enterocin W, a novel two-peptide lantibiotic produced by Enterococcus faecalis NKR-4-1. *Applied and Environmental Microbiology*. **78**, 900–903

9. Haas, W., Shepard, B. D., and Gilmore, M. S. (2002) Two-component regulator of Enterococcus faecalis cytolysin responds to quorum-sensing autoinduction. *Nature*. **415**, 84–87

551 10. Inoue, T., Tomita, H., and Ike, Y. (2006) Bac 32, a novel bacteriocin widely
552 disseminated among clinical isolates of Enterococcus faecium. *Antimicrobial Agents and*
553 *Chemotherapy*. **50**, 1202–1212

554 11. Martínez-Bueno, M., Maqueda, M., Galvez, A., Samyn, B., Beeumen, J. V., Coyette, J.,
555 and Valdivia, E. (1994) Determination of the gene sequence and the molecular structure of
556 the enterococcal peptide antibiotic AS-48. *Journal of bacteriology*. **176**, 6334–6339

557 12. Todokoro, D., Tomita, H., Inoue, T., and Ike, Y. (2006) Genetic analysis of bacteriocin
558 43 of vancomycin-resistant Enterococcus faecium. *Applied and Environmental*
559 *Microbiology*. **72**, 6955–6964

560 13. Tomita, H., Fujimoto, S., Tanimoto, K., and Ike, Y. (1997) Cloning and genetic and
561 sequence analyses of the bacteriocin 21 determinant encoded on the Enterococcus faecalis
562 pheromone-responsive conjugative plasmid pPD1. *Journal of bacteriology*. **179**, 7843–
563 7855

564 14. Tomita, H., Fujimoto, S., Tanimoto, K., and Ike, Y. (1996) Cloning and genetic
565 organization of the bacteriocin 31 determinant encoded on the Enterococcus faecalis
566 pheromone-responsive conjugative plasmid pYI17. *Journal of bacteriology*. **178**, 3585–
567 3593

568 15. Yamashita, H., Tomita, H., Inoue, T., and Ike, Y. (2011) Genetic organization and
569 mode of action of a novel bacteriocin, Bacteriocin 51: determinant of VanA-type
570 vancomycin-resistant Enterococcus faecium. *Antimicrobial Agents and Chemotherapy*. **55**,
571 4352–4360

572 16. Nilsen, T., Nes, I. F., and Holo, H. (2003) Enterolysin A, a cell wall-degrading
573 bacteriocin from Enterococcus faecalis LMG 2333. *Applied and Environmental*
574 *Microbiology*. **69**, 2975–2984

575 17. Tomita, H., Kamei, E., and Ike, Y. (2008) Cloning and genetic analyses of the
576 bacteriocin 41 Determinant encoded on the Enterococcus faecalis pheromone-responsive
577 conjugative plasmid pYI14: a novel bacteriocin complemented by two extracellular
578 components (lysin and activator). *Journal of bacteriology*. **190**, 2075–2085

18. Kurushima, J., Ike, Y., and Tomita, H. (2016) Partial diversity generates effector-immunity specificity of the Bac41-like bacteriocins of Enterococcus faecalis clinical strains. *Journal of bacteriology*. 10.1128/jb.00348-16

19. Zheng, B., Tomita, H., Inoue, T., and Ike, Y. (2009) Isolation of VanB-type Enterococcus faecalis strains from nosocomial infections: first report of the isolation and identification of the pheromone-responsive plasmids pMG2200, encoding VanB-type vancomycin resistance and a Bac41-type bacteriocin, and pMG2201, encoding erythromycin resistance and cytolysin (Hly/Bac). *Antimicrobial Agents and Chemotherapy*. **53**, 735–747

20. Kurushima, J., Nakane, D., Nishizaka, T., and Tomita, H. (2015) Bacteriocin Protein BacL1 of Enterococcus faecalis Targets Cell Division Loci and Specifically Recognizes l-Ala2-Cross-Bridged Peptidoglycan. *Journal of bacteriology*. **197**, 286–295

21. Tomita, H., Todokoro, D., and Ike, Y. (2010) Genetic analysis of the bacteriocin 41 encoded on the Enterococcus faecalis pheromone-responsive conjugative plasmid pYI14. *3rd International ASM Conference on Enterococci, Abstr. 30B, pp. 37–38, American Society for Microbiology, Washington, D. C.*

22. Kurushima, J., Hayashi, I., Sugai, M., and Tomita, H. (2013) Bacteriocin protein BacL1 of Enterococcus faecalis is a peptidoglycan D-isoglutamyl-L-lysine endopeptidase. *Journal of Biological Chemistry*. **288**, 36915–36925

23. Bonofiglio, L., García, E., and Mollerach, M. (2005) Biochemical Characterization of the Pneumococcal Glucose 1-Phosphate Uridylyltransferase (GalU) Essential for Capsule Biosynthesis. *Curr Microbiol*. **51**, 217–221

24. Mendicino, J. (1960) Sucrose phosphate synthesis in wheat germ and green leaves. *The Journal of biological chemistry*. **235**, 3347–3352

25. Neves, A. R., Pool, W. A., Solopova, A., Kok, J., Santos, H., and Kuipers, O. P. (2010) Towards enhanced galactose utilization by Lactococcus lactis. *Applied and Environmental Microbiology*. **76**, 7048–7060

26. Berbis, M., Sanchez-Puelles, J., Canada, F., and Jimenez-Barbero, J. (2015) Structure and Function of Prokaryotic UDP-Glucose Pyrophosphorylase, A Drug Target Candidate. *Curr Med Chem*. **22**, 1687–1697

609 27. Guerardel, Y., Sadovskaya, I., Maes, E., Furlan, S., Chapot-Chartier, M.-P., Mesnage,
610 S., Rigottier-Gois, L., and Serror, P. (2020) Complete Structure of the Enterococcal
611 Polysaccharide Antigen (EPA) of Vancomycin-Resistant Enterococcus faecalis V583
612 Reveals that EPA Decorations Are Teichoic Acids Covalently Linked to a
613 Rhamnopolysaccharide Backbone. *Mbio*. 10.1128/mbio.00277-20

614 28. Thurlow, L. R., Thomas, V. C., and Hancock, L. E. (2009) Capsular polysaccharide
615 production in Enterococcus faecalis and contribution of CpsF to capsule serospecificity.
616 *Journal of bacteriology*. **191**, 6203–6210

617 29. Teng, F. (2002) Evidence that the Enterococcal Polysaccharide Antigen Gene (epa)
618 Cluster Is Widespread in Enterococcus faecalis and Influences Resistance to Phagocytic
619 Killing of E. faecalis. *Infection and immunity*. **70**, 2010–2015

620 30. Teng, F., Singh, K. V., Bourgogne, A., Zeng, J., and Murray, B. E. (2009) Further
621 characterization of the epa gene cluster and Epa polysaccharides of Enterococcus faecalis.
622 *Infection and immunity*. **77**, 3759–3767

623 31. Dale, J. L., Cagnazzo, J., Phan, C. Q., Barnes, A. M. T., and Dunny, G. M. (2015)
624 Multiple roles for Enterococcus faecalis glycosyltransferases in biofilm-associated
625 antibiotic resistance, cell envelope integrity, and conjugative transfer. *Antimicrobial Agents*
626 *and Chemotherapy*. **59**, 4094–4105

627 32. Xu, Y., Murray, B. E., and Weinstock, G. M. (1998) A cluster of genes involved in
628 polysaccharide biosynthesis from Enterococcus faecalis OG1RF. *Infection and immunity*.
629 **66**, 4313–4323

630 33. Korir, M. L., Dale, J. L., and Dunny, G. M. (2019) Role of epaQ, a Previously
631 Uncharacterized Enterococcus faecalis Gene, in Biofilm Development and Antimicrobial
632 Resistance. *J Bacteriol*. 10.1128/jb.00078-19

633 34. Chatterjee, A., Johnson, C. N., Luong, P., Hullahalli, K., McBride, S. W., Schubert, A.
634 M., Palmer, K. L., Carlson, P. E., and Duerkop, B. A. (2019) Bacteriophage Resistance
635 Alters Antibiotic-Mediated Intestinal Expansion of Enterococci. *Infect Immun*.
636 10.1128/iai.00085-19

637 35. Singh, K. V., and Murray, B. E. (2019) Loss of a Major Enterococcal Polysaccharide
638 Antigen (Epa) by Enterococcus faecalis Is Associated with Increased Resistance to
639 Ceftriaxone and Carbapenems. *Antimicrob Agents Ch*. 10.1128/aac.00481-19

640 36. Thoden, J. B., and Holden, H. M. (2007) The molecular architecture of glucose-1-
641 phosphate uridylyltransferase. *Protein science : a publication of the Protein Society*. **16**,
642 432–440

643 37. Aragão, D., Fialho, A. M., Marques, A. R., Mitchell, E. P., Sá-Correia, I., and Frazão,
644 C. (2007) The complex of Sphingomonas elodea ATCC 31461 glucose-1-phosphate
645 uridylyltransferase with glucose-1-phosphate reveals a novel quaternary structure, unique
646 among nucleoside diphosphate-sugar pyrophosphorylase members. *Journal of bacteriology*.
647 **189**, 4520–4528

648 38. Bentley, S. D., Aanensen, D. M., Mavroidi, A., Saunders, D., Rabbinowitsch, E.,
649 Collins, M., Donohoe, K., Harris, D., Murphy, L., Quail, M. A., Samuel, G., Skovsted, I.
650 C., Kaltoft, M. S., Barrell, B., Reeves, P. R., Parkhill, J., and Spratt, B. G. (2006) Genetic
651 Analysis of the Capsular Biosynthetic Locus from All 90 Pneumococcal Serotypes. *PLOS*
652 *Genetics*. **2**, e31-8

653 39. Prasad, S. B., Jayaraman, G., and Ramachandran, K. B. (2010) Hyaluronic acid
654 production is enhanced by the additional co-expression of UDP-glucose pyrophosphorylase
655 in Lactococcus lactis. *Applied microbiology and biotechnology*. **86**, 273–283

656 40. Mollerach, M., López, R., and García, E. (1998) Characterization of the galU gene of
657 Streptococcus pneumoniae encoding a uridine diphosphoglucose pyrophosphorylase: a
658 gene essential for capsular polysaccharide biosynthesis. *The Journal of experimental*
659 *medicine*. **188**, 2047–2056

660 41. Hardy, G. G., Caimano, M. J., and Yother, J. (2000) Capsule biosynthesis and basic
661 metabolism in Streptococcus pneumoniae are linked through the cellular
662 phosphoglucomutase. *Journal of bacteriology*. **182**, 1854–1863

663 42. Maekawa, S., Yoshioka, M., and Kumamoto, Y. (1992) Proposal of a new scheme for
664 the serological typing of Enterococcus faecalis strains. **36**, 671–681

665 43. Hufnagel, M., Hancock, L. E., Koch, S., Theilacker, C., Gilmore, M. S., and Huebner,
666 J. (2004) Serological and genetic diversity of capsular polysaccharides in Enterococcus
667 faecalis. *Journal of Clinical Microbiology*. **42**, 2548–2557

668 44. Hancock, L. E., and Gilmore, M. S. (2002) The capsular polysaccharide of
669 Enterococcus faecalis and its relationship to other polysaccharides in the cell wall.
670 *Proceedings of the National Academy of Sciences of the United States of America*. **99**,
671 1574–1579

672 45. Rigottier-Gois, L., Alberti, A., Houel, A., Taly, J.-F., Palcy, P., Manson, J., Pinto, D.,
673 Matos, R. C., Carrilero, L., Montero, N., Tariq, M., Karsens, H., Repp, C., Kropec, A.,
674 Budin-Verneuil, A., Benachour, A., Sauvageot, N., Bizzini, A., Gilmore, M. S., Bessières,
675 P., Kok, J., Huebner, J., Lopes, F., Gonzalez-Zorn, B., Hartke, A., and Serror, P. (2011)
676 Large-Scale Screening of a Targeted Enterococcus faecalis Mutant Library Identifies
677 Envelope Fitness Factors. *PloS one*. **6**, e29023-10

678 46. Weart, R. B., Lee, A. H., Chien, A.-C., Haeusser, D. P., Hill, N. S., and Levin, P. A.
679 (2007) A metabolic sensor governing cell size in bacteria. *Cell*. **130**, 335–347

680 47. Cho, H., Uehara, T., and Bernhardt, T. G. (2014) Beta-lactam antibiotics induce a lethal
681 malfunctioning of the bacterial cell wall synthesis machinery. *Cell*. **159**, 1300–1311

682 48. Dunny, G. M., Craig, R. A. R., Carron, R. L. R., and Clewell, D. B. (1979) Plasmid
683 transfer in Streptococcus faecalis: production of multiple sex pheromones by recipients.
684 *Plasmid*. **2**, 454–465

685 49. Fujimoto, S., and Ike, Y. (2001) pAM401-based shuttle vectors that enable
686 overexpression of promoterless genes and one-step purification of tag fusion proteins
687 directly from Enterococcus faecalis. *Applied and Environmental Microbiology*. **67**, 1262–
688 1267

689 50. Bryan, E. M., Bae, T., Kleerebezem, M., and Dunny, G. M. (2000) Improved Vectors
690 for Nisin-Controlled Expression in Gram-Positive Bacteria. *Plasmid*. **44**, 183–190

691 51. Kristich, C. J., Chandler, J. R., and Dunny, G. M. (2007) Development of a host-
692 genotype-independent counterselectable marker and a high-frequency conjugative delivery
693 system and their use in genetic analysis of Enterococcus faecalis. *Plasmid*. **57**, 131–144

694 52. Schindelin, J., Arganda-Carreras, I., Frise, E., Kaynig, V., Longair, M., Pietzsch, T.,
695 Preibisch, S., Rueden, C., Saalfeld, S., Schmid, B., Tinevez, J.-Y., White, D. J.,
696 Hartenstein, V., Eliceiri, K., Tomancak, P., and Cardona, A. (2012) Fiji: an open-source
697 platform for biological-image analysis. *Nature methods*. **9**, 676–682

698 53. Paintdakhi, A., Parry, B., Campos, M., Irnov, I., Elf, J., Surovtsev, I., and Jacobs-
699 Wagner, C. (2016) Oufti: an integrated software package for high-accuracy, high-
700 throughput quantitative microscopy analysis. *Molecular microbiology*. **99**, 767–777

701 54. Raaphorst, R. van, Kjos, M., and Veening, J.-W. (2020) BactMAP: An R package for
702 integrating, analyzing and visualizing bacterial microscopy data. *Molecular microbiology*.
703 **11**, 2699

704 55. Villanueva, R. A. M., and Chen, Z. J. (2019) ggplot2: Elegant Graphics for Data
705 Analysis (2nd ed.). *Meas Interdiscip Res Perspectives*. **17**, 160–167

706

Table 1 Bacterial strains and plasmids used in this study

	Descriptions	References
Strains		
E. faecalis		
OG1S	*str*^{r}, derivative of OG1	20
OG1S::*galU*^{C862T}	Isogenic mutant of OG1S carrying the point mutation in *galU*	This study
CK111	Donor for conjugation of pCJK47 derivatives	23
OG1RF	*rif*^{r}, *fus*^{r}, derivative of OG1	20
OG1RF*ΔgalU*	Isogenic mutant of OG1RF carrying the in-frame deletion of *galU*	This study
OG1RF*ΔepaB*	Isogenic mutant of OG1RF carrying the in-frame deletion of *epaB*	This study
FA2-2	*rif*^{r}, *fus*^{r}, derivative of JH2	20
FA2-2*ΔgalU*	Isogenic mutant of FA2-2 carrying the in-frame deletion of *galU*	This study
E. coli		
DH5α	Host for DNA cloning	Bethesda Research Laboratories
BL21 Rosetta	Host for protein expression	Novagen
EC1000	Host for cloning of pCJK47 derivatives	23
Plasmids		
pMGS100	*E. coli*-*E. faecalis* shuttle expression plasmid; *cat*	49
p*galU*	pMGS100 containing *galU* gene	This study
pCF10-101	Helper plasmid for conjugation of pCJK47 derivatives	51
pCJK47	Suicide vector for construction of deletion mutants	51
pCJK47::*ΔgalU*	pCJK47 containing in-frame deletion of *galU* and its flanking region	This study
pCJK47::*ΔepaB*	pCJK47 containing in-frame deletion of *epaB* and its flanking region	This study
pMSP3535	*E. coli*-*E. faecalis* shuttle nisin-inducible expression plasmid; *erm*	50
p*epaB*	pMSP3535 containing *epaB* gene	This study
pET22(+)	Expression vector of His-tagged protein in *E. coli*	Novagen
pET22::*bacL1*	pET22b (+) containing *bacL*$_1$ gene derived from pYI14	22
pET22::*bacA*	pET22b (+) containing *bacA* gene derived from pYI14	22
Oligonucleotides[a]		
F-*galU*_del_up	ccggaattcCCTGGGGGACAGCTTTAGCT	This study
R-*galU*-del_up	ctctttttttcgcTGCTGGAATAACTGCCTTTT	This study
F-*galU*_del_dwn	gttattccagcaGCGAAAAAAGAGCAACCAAA	This study
R-*galU*-del_dwn	ccggaattcCTTGAGCATCGTCAGCTGCT	This study
F-*galU*-pMGS	ttttgaggaggcggcATGAAAGTTAAAAAGGCAGT	This study
R-*galU*-pMGS	gcgtcgatcttatcgTTATTTTTCTTTTGGTTGCT	This study
F-*epaB*_del_up	ccatacggaattcGGATAGATTTTGTG	This study
R-*epaB*-del_up	atttgttaaaCGAGATTGTTACCATTTCTT	This study
F-*epaB*_del_dwn	aacaatctcgTTTAACAAATGGGGCTGGAG	This study
R-*epaB*-del_dwn	ccatacggaattcGAATACTATCTAATTGTTCC	This study
F-*epaB*-pMSP3535	gactctgcatggatcATGAGCATGCAAGAAATGGT	This study
R-*epaB*-pMSP3535	tagtggtaccggatcTTAAAAGAACCTCCAGCCCC	This study

[a]Lowercase letters indicate additional nucleotides for enzyme digestion, overlap PCR or seemless cloning.

Table 2 MICs of antimicrobial drugs for *E. faecalis* strains (mg/L)

	ABPC	PEN	VAN	GEN	DAP	SDS
OG1S WT	2	2	4	16	1	250
OG1S *galU*^{C862T}	4	4	2	4	<0.125	125
OG1S *galU*^{C862T}/Vec	4	4	2	4	<0.125	125
OG1S *galU*^{C862T}/p*galU*	2	2	4	16	1	250
OG1RF WT	2	2	4	16	1	250
OG1RF *ΔgalU*	4	4	2	8	<0.125	125
OG1RF *ΔepaB*	4	4	2	16	1	125

ABPC, ampicillin; PEN, penicillin; VAN, vancomycin; GEN, gentamicin; DAP, daptomycin; SDS, sodium dodecyl sulfate

Fig. 1

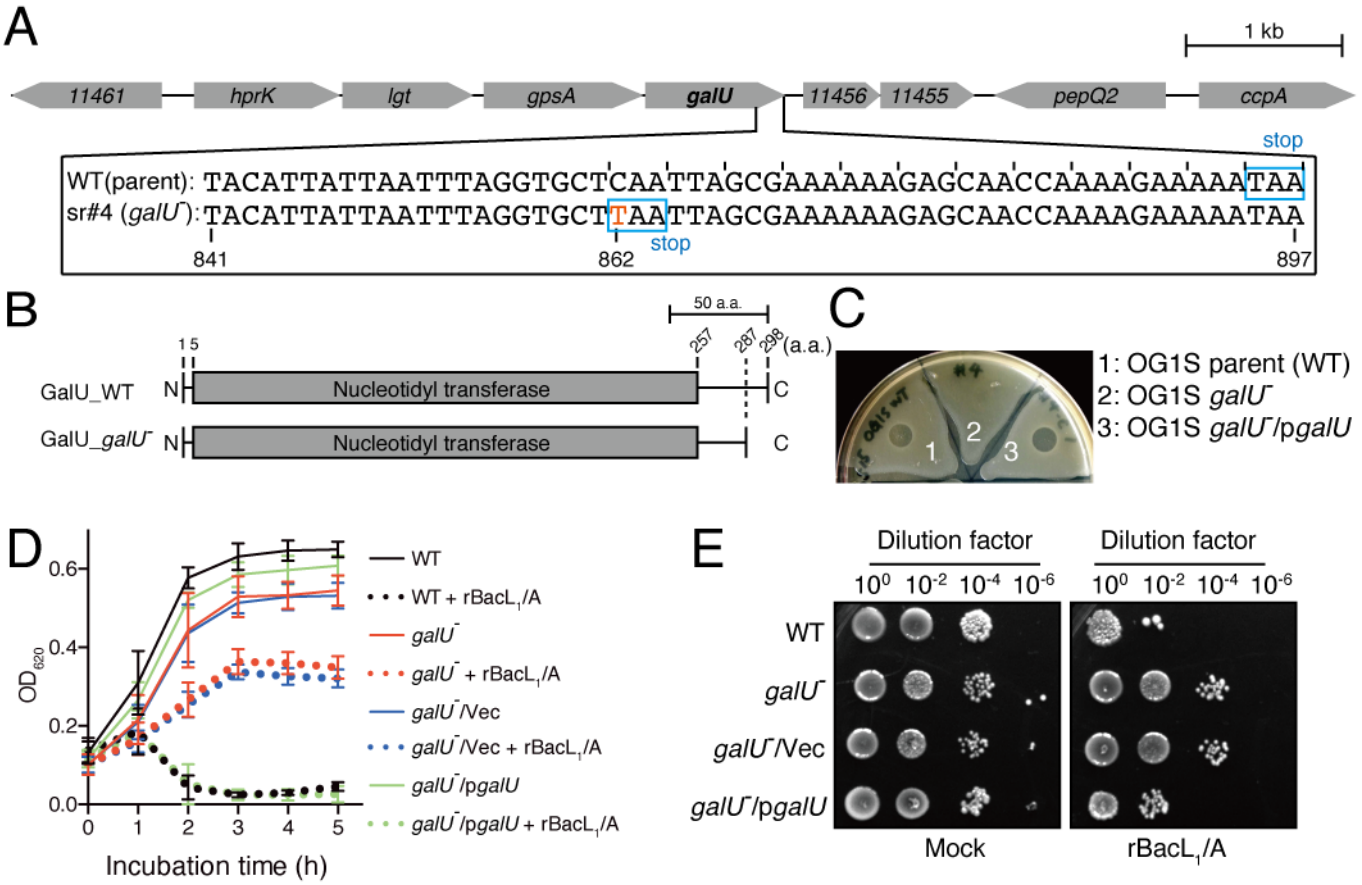

Figure 1. Genetic mutation found in the strain spontaneously resistant to the antimicrobial activity of Bac41. (A) Nucleotide sequence alignment of the *galU* (OG1RF_11457; Gene ID: 12287400) genes of the *E. faecalis* OG1S parent strain (upper) and the OG1S isogenic mutant strain (sr#4) that spontaneously acquired resistance to the antimicrobial activity of Bac41 (lower). Scale bar, 1 kb. (B) Amino acid sequence alignment of the translation products of the *galU* genes of the *E. faecalis* OG1S parent strain (upper) and the OG1S isogenic mutant strain (lower). Scale bar, 50 a.a.. (C) A mixture of recombinant $BacL_1$-His and BacA-His proteins (25 ng each) was spotted onto THB soft agar (0.75%) containing the indicator strain *E. faecalis* OG1S (Parent, 1), the spontaneously resistant strain with the *galU* mutation (*galU*-, 2), and the *galU*- strain complemented via the trans-expression of wild-type GalU from the p*galU* plasmid (*galU*-/p*galU*, 3). The plate was incubated at 37 °C for 24 h, and the formation of halos was evaluated. (D) Overnight cultures of *E. faecalis* strains, including OG1S (WT), the *galU* mutant (*galU*-), the vector control strain of *galU*- (*galU*-/Vec) and the complemented *galU*- strain (*galU*-/p*galU*), were inoculated into fresh THB broth at a 5-fold dilution. A mixture of recombinant $BacL_1$-His (5 μg/ml) and BacA-His (5 μg/ml) was added to the bacterial suspension and incubated at 37 °C. The turbidity was monitored during the incubation period. The data for each case are presented as the mean ±S.D. (error bars) of three independent experiments. (E) The *E. faecalis* strains were treated with $rBacL_1$ and BacA (5 μg/ml each) at 37 °C for 4 h, as described in panel D. The bacterial suspensions were serially diluted 100-fold with fresh THB and then spotted onto a THB agar plate, followed by incubation overnight. Colony formation was evaluated as a measure of bacterial viability.

Fig. 2

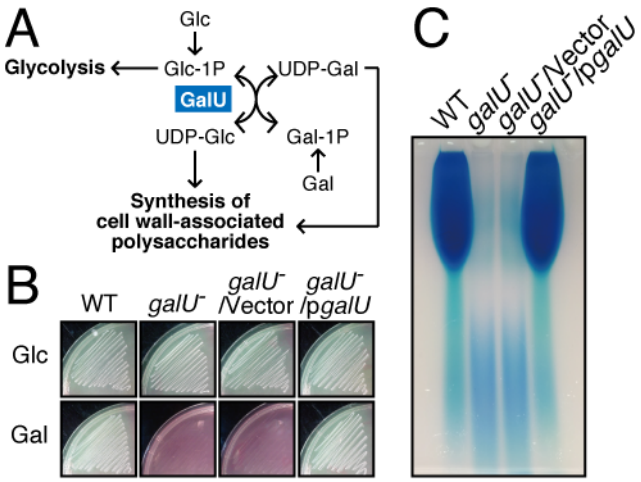

Figure 2. *galU* is essential for galactose fermentation and cell surface polysaccharide production. (A) The Leloir pathway of galactose metabolism is illustrated. GalU generates UDP-glucose (UDP-Glc) from glucose-1-phosphate (Glc-1P) and ATP. (B) The *E. faecalis* wild-type, *galU*$^-$, *galU*$^-$/Vec and *galU*$^-$/p*galU* strains were grown in HI agar medium supplemented with phenol red as a pH indicator and glucose (Glc) or galactose (Gal) as the fermentation source. (C) The *E. faecalis* wild-type, *galU*$^-$, *galU*$^-$/Vec and *galU*$^-$/p*galU* strains were grown in THB broth supplemented with glucose, and the cell wall-associated polysaccharides were prepared as described in the Materials and Methods section. The resulting polysaccharides were separated via 10% acrylamide gel electrophoresis, followed by staining with the Stains-All reagent.

Fig. 3

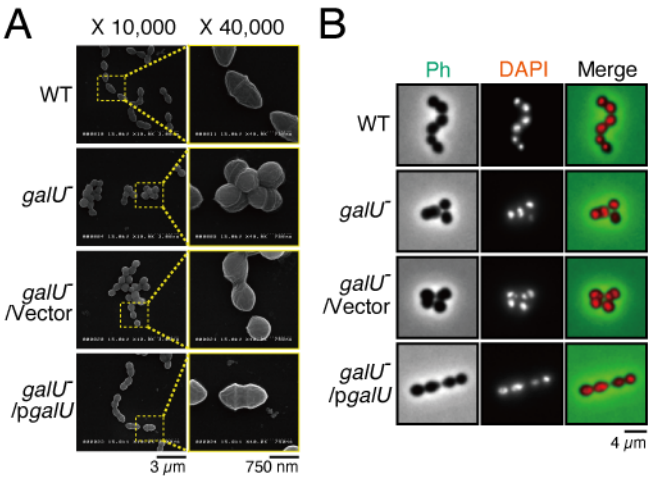

Figure 3. *galU* is essential for maintaining cell morphology. (A) The *E. faecalis* wild-type, *galU*$^-$, *galU*$^-$/Vec and *galU*$^-$/p*galU* strains were grown on cover glasses, followed by chemical fixation. The samples were subjected to osmium coating and analyzed under the scanning electron microscope. Scale bars, 3 μm (left) and 750 nm (right). (B) Overnight cultures of the *E. faecalis* wild-type, *galU*$^-$, *galU*$^-$/Vec and *galU*$^-$/p*galU* strains were diluted 5-fold with fresh THB broth and incubated, chemically fixed and mounted with DAPI for DNA visualization (red), followed by analysis via fluorescence microscopy. Phase contrast (Ph) is pseudocolored (green) in the merged image. Scale bar, 4 μm.

Fig. 4

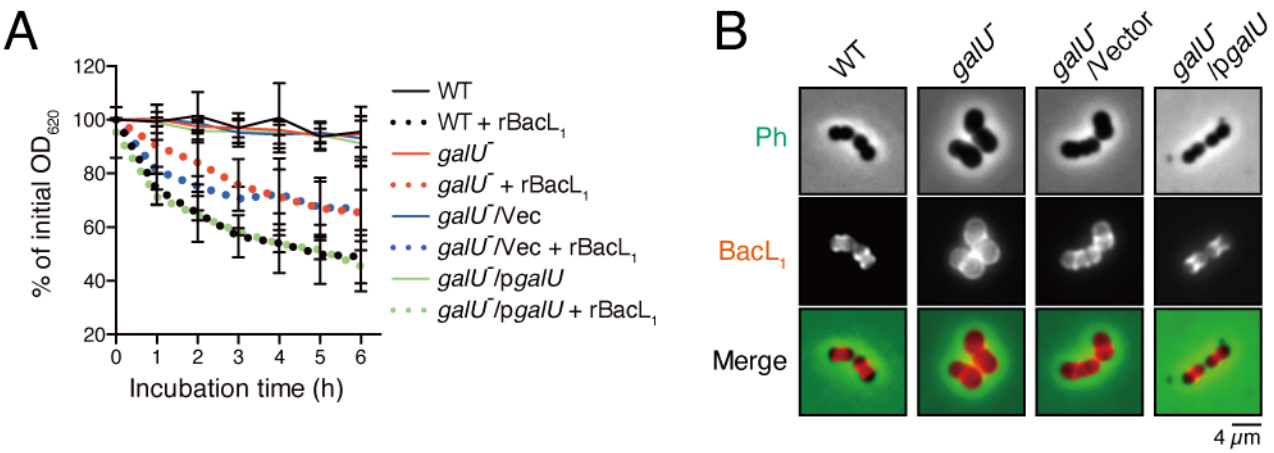

Figure 4. *galU* inactivation alters the interaction of $BacL_1$ with the cell wall of *E. faecalis*. (A) Cell wall fractions prepared from *E. faecalis* wild-type (black), *galU*⁻ (red), *galU*⁻/Vec (blue) and *galU*⁻/p*galU* (green) in exponential phase were diluted with PBS. Recombinant $BacL_1$ ($rBacL_1$, 5 μg/ml, dotted lines) was added to the cell wall suspension, and the mixture was incubated at 37 °C. The turbidity at 600 nm was quantified at the indicated times during incubation. The presented values are the percentages of the initial turbidity for the respective samples. The PBS-treated sample (mock) is presented as a negative control (straight lines). The data are presented as the mean ±S.D. (error bars) of four independent experiments. (B) Overnight cultures of the *E. faecalis* wild-type, *galU*⁻, *galU*⁻/Vec and *galU*⁻/p*galU* strains were diluted 5-fold with fresh THB broth and incubated with HiLyte Fluor 555 fluorescent dye-labeled (red) $BacL_1$ (5 μg/ml), followed by analysis via fluorescence microscopy. Phase contrast (Ph) is pseudocolored (green) in the merged images. Scale bar, 4 μm.

Fig. 5

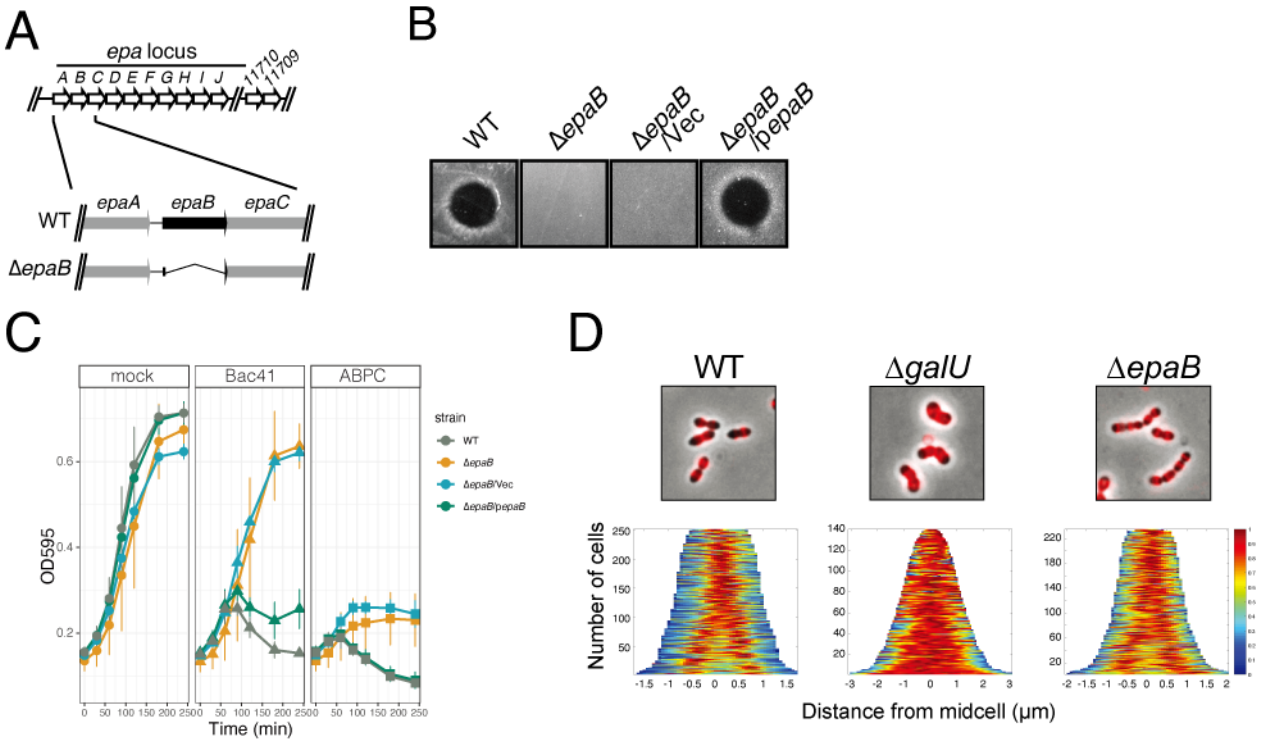

Figure 5. Effect of *epaB* deletion on the binding affinity of BacL$_1$ and susceptibility to Bac41 activity. (A) Genomic organization of the *epa* locus in *E. faecalis* OG1RF and construction of an *epaB*-deletion mutant. (B) A mixture of the recombinant BacL$_1$-His and BacA-His proteins (25 ng each) was spotted onto THB soft agar (0.75%) containing the indicator strain *E. faecalis* wild type, *ΔepaB*, *ΔepaB*/Vec and *ΔepaB*/p*epaB* strains. The plate was incubated at 37 °C for 24 h, and the formation of halos was evaluated. (C) The overnight cultures of the *E. faecalis* strains OG1RF (WT), Δ*epaB*, Δ*epaB*/Vec and Δ*epaB*/p*epaB* were inoculated into fresh THB broth at a 10-fold dilution in the presence or absence of ABPC (4 mg/L) or Bac41 (BacL1 and BacA, 2.5 μg/mL each), followed by incubation at 37 °C. The turbidity (OD_{595}) was monitored during the incubation period. The data for each case are presented as the % of the initial turbidity. The data are presented as the mean ±S.D. (error bars) of three independent experiments.(D) Overnight cultures of the *E. faecalis* wild-type, Δ*galU* and Δ*epaB* strains were diluted 5-fold with fresh THB broth and incubated with HiLyte Fluor 555 fluorescent dye-labeled (red) BacL$_1$_SH3-His (5 μg/ml), followed by analysis via fluorescence microscopy.

Fig. 6

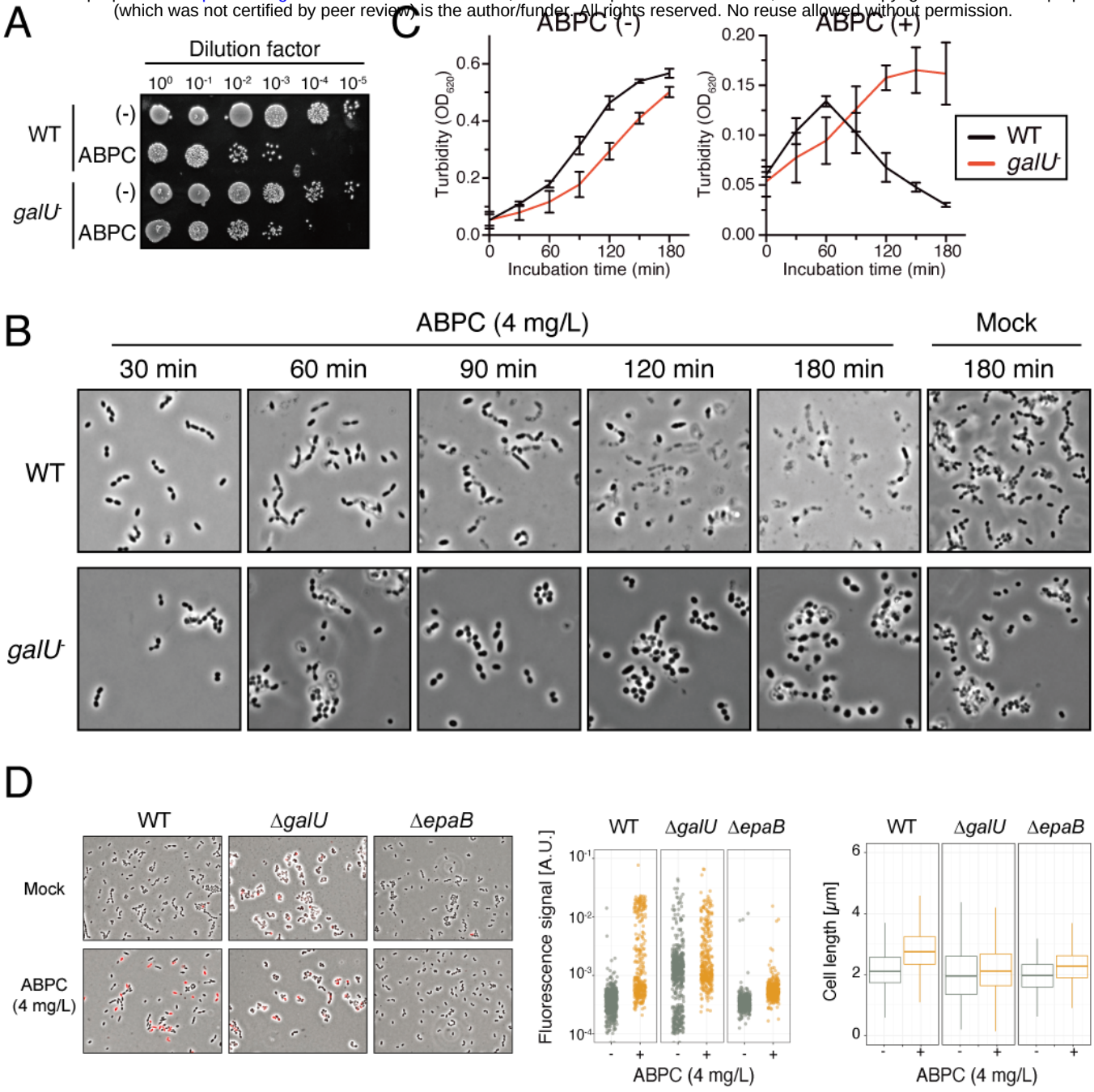

Figure 6. Different bacteriolysis phenotypes induced by ampicillin treatment (ABPC) in the *E. faecalis* wild-type strain or the *galU*- mutant. (A) The *E. faecalis* strains OG1S (WT) and the *galU*- mutant were treated with ABPC (4 mg/L) at 37 °C for 3 h. The bacterial suspensions were serially diluted 10-fold with fresh THB and then spotted onto a THB agar plate, followed by incubation overnight. Colony formation was evaluated as a measure of bacterial viability. (B) Confluent cultures of the *E. faecalis* OG1S (WT) and *galU*- strains were diluted 10-fold with fresh THB containing ABPC(4 mg/L), followed by incubation at 37°C. The bacterial suspension was mounted onto a slide and analyzed via microscopy (phase contrast) at the indicated time points: 30, 60, 90, 120 and 180 min after treatment. The yellow arrowheads indicate the cell debris generated by ABPC-induced bacteriolysis. Cells incubated under identical conditions except for the absence of ABPC (Mock) are represented in the right panel as a reference. Scale bar, 20 μm. (C) The overnight cultures of the *E. faecalis* strains OG1S (WT) and *galU*- were inoculated into fresh THB broth at a 10-fold dilution in the presence or absence of ABPC(4 mg/L), followed by incubation at 37 °C. The turbidity was monitored during the incubation period. The data for each case are presented as the % of the initial turbidity. The data are presented as the mean ±S.D. (error bars) of three independent experiments. (D) The overnight cultures of the *E. faecalis* strains OG1RF (WT), Δ*galU* and Δ *epaB* were inoculated into fresh THB broth at a 10-fold dilution in the presence or absence of ABPC (4 mg/L), followed by incubation at 37°C for 1 h with EthD (2 mg/L). The bacterial suspension was mounted onto a slide and analyzed via fluorescence microscopy. Images are shown as merge of phase contrast and red fluorescence signal (EthD). (E and F) Quantification of population with red fluorescence intensity (E) and cell length (F) on each celll was generated images of based on panel D.

Fig. S1

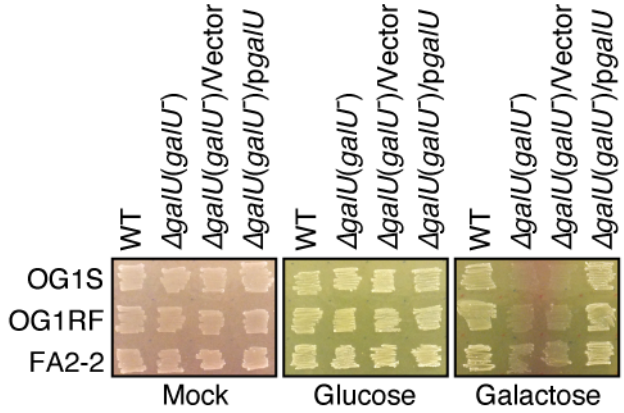

Supplementary figure S1. Effect of the *galU* inactivation on glucose or galactose fermentation. The indicated *E. faecalis* strains were grown in HI agar media that was supplemented with phenol red as a pH indicator and glucose or galactose as the fermentation source, respectively.

Fig. S2

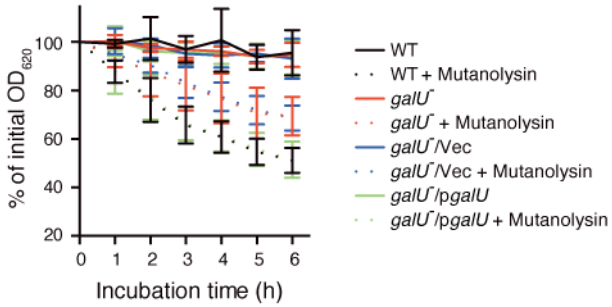

Supplementary figure S2. Susceptibility of cell wall derived from the *E. faecalis* strains to Mutanolysin. Cell wall fractions prepared from *E. faecalis* wild type (black), *galU*⁻ (red), *galU*⁻/Vec (blue) and *galU*⁻/p*galU* (green) in exponential phase were diluted with PBS. Mutanolysin (1 μg/ml, dotted lines) was added to the cell wall suspension, and the mixture was incubated at 37°C. The turbidity at 620 nm was quantified at the indicated times during incubation. The present values are the percentages of the initial turbidity for the respective samples. The PBS treated sample (mock) is presented as a negative control (straight lines). The data are presented as the mean ±S.D. (error bars) of four independent experiments.

Fig. S3

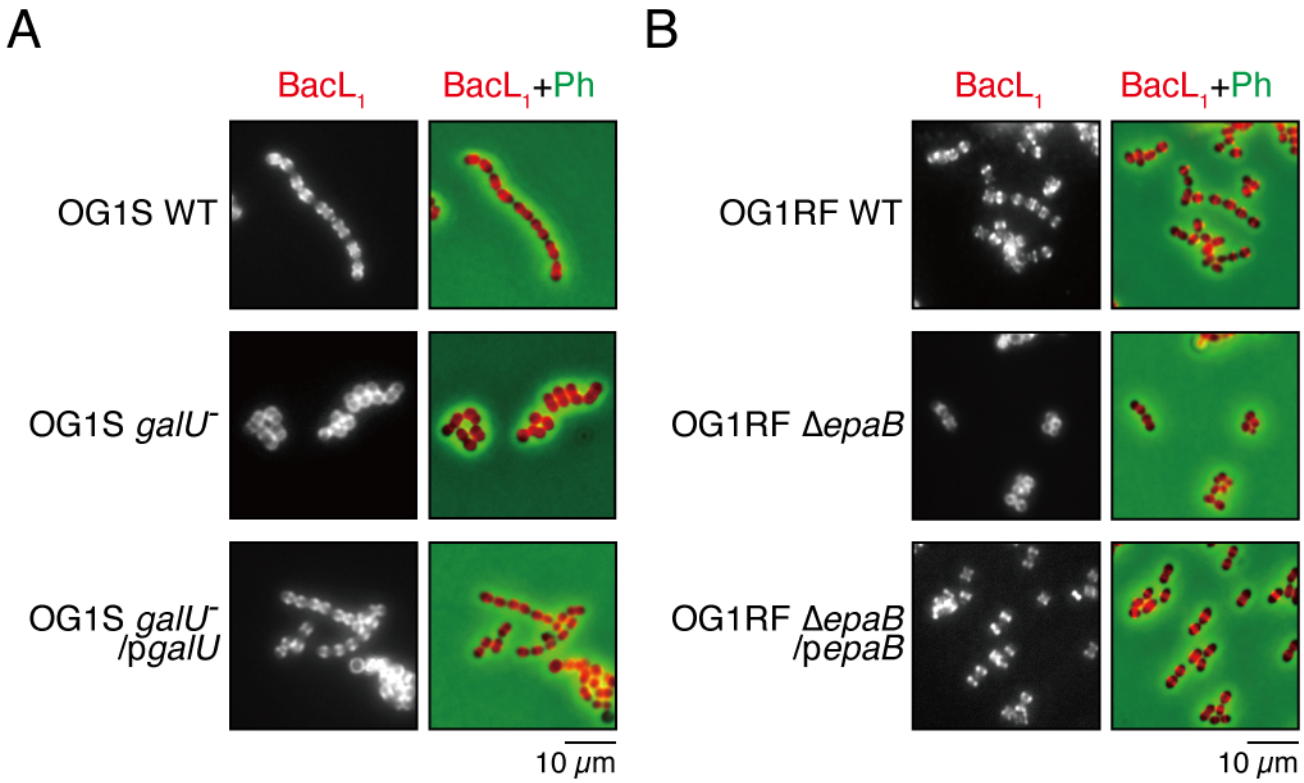

Supplementary figure S3. Overnight cultures of *E. faecalis* OG1S wild type, *galU*$^-$ and *galU*$^-$/p*galU*$^-$ strains (A) or *E. faecalis* OG1RF wild type, *ΔepaB* and *ΔepaB*/p*epaB* strains (B) were diluted 5-fold with fresh THB broth, and were incubated with the HiLyte Fluor 555 fluorescent dye-labeled (red) $BacL_1$ (5 μg/ml), followed by analysis using fluorescence microscopy. Phase contrast (Ph) is pseudocolored (green) in merged images. These image in panel A or B are wide-field versions of the magnificated fluorescent images represented in Fig. 4B or Fig. 5D, respectively. Scale bar; 10 μm.

Fig. S4

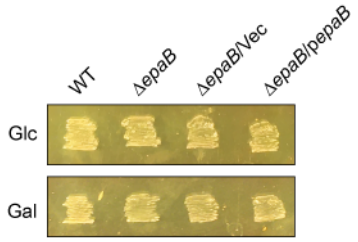

Supplementary figure S4. Effect of the *epaB* inactivation on glucose or galactose fermentation. The indicated *E. faecalis* strains were grown in HI agar media that was supplemented with phenol red as a pH indicator and glucose (Glc) or galactose (Gal) as the fermentation source, respectively.

Fig. S5

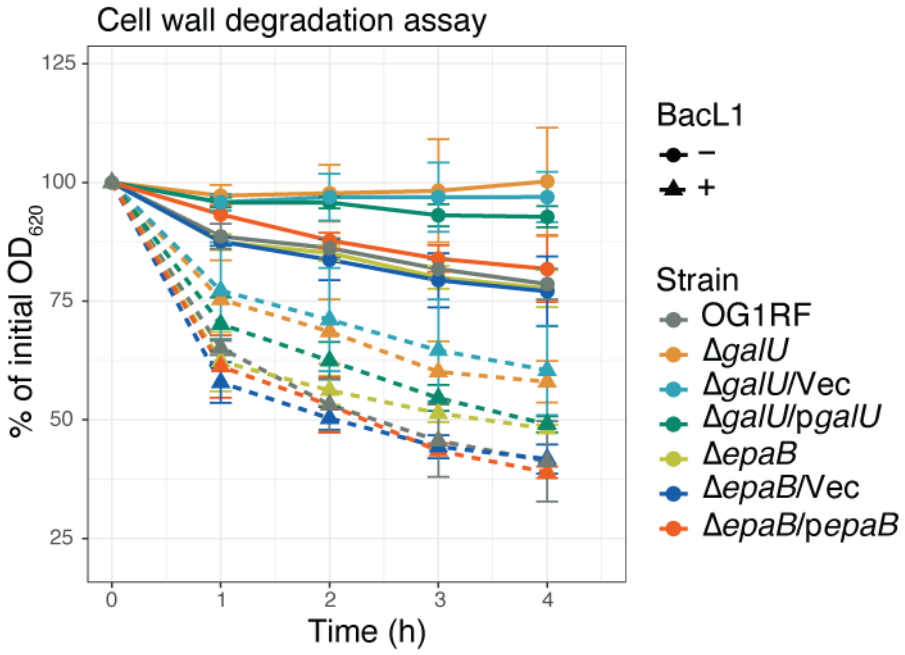

Supplementary figure S5. Susceptibility of cell wall derived from the *E. faecalis* strains to recombinant $BacL_1$. Cell wall fractions prepared from *E. faecalis* wild type, Δ*galU*, Δ*galU*/Vec, Δ*galU*/p*galU*, Δ*epaB*, Δ*epaB*/Vec and Δ*epaB*/p*epaB* in exponential phase were diluted with PBS. $BacL_1$-His (5 μg/ml) was added to the cell wall suspension, and the mixture was incubated at 37°C. The turbidity at 620 nm was quantified at the indicated times during incubation. The present values are the percentages of the initial turbidity for the respective samples. The PBS treated sample (mock) is presented as a negative control (straight lines). The data are presented as the mean ±S.D. (error bars) of four independent experiments.

Fig. S6

Figure S6. Alignment of the amino acid sequences of GalU homologues (GalU/HasC) from various Gram-positive bacterial species. The deleted region in the *galU*- strain used in this study is surrounded by a red frame. Source strains and GI numbers: *E. faecalis* OG1S/OG1RF (GI:327535310); *Enterococcus faecalis* JH2-2 (GI:551092274); *Enterococcus faecium* DO (GI:389869192); *Enterococcus hirae* ATCC9790 (GI:498408730); *Streptococcus suis* BM407 (GI:253756447); *Streptococcus pneumoniae* D39 (GI:116076768); *Streptococcus mutans* UA159 (GI:24378821); *Streptococcus intermedius* B196 (GI:538452117); *Streptococcus dysgalactiae* AC-2713 (GI:489151789); *Streptococcus agalactiae* 2603V R (GI:22536589); and *Streptococcus pyogenes* M1 GAS (GI:15674413).

Fig. S7

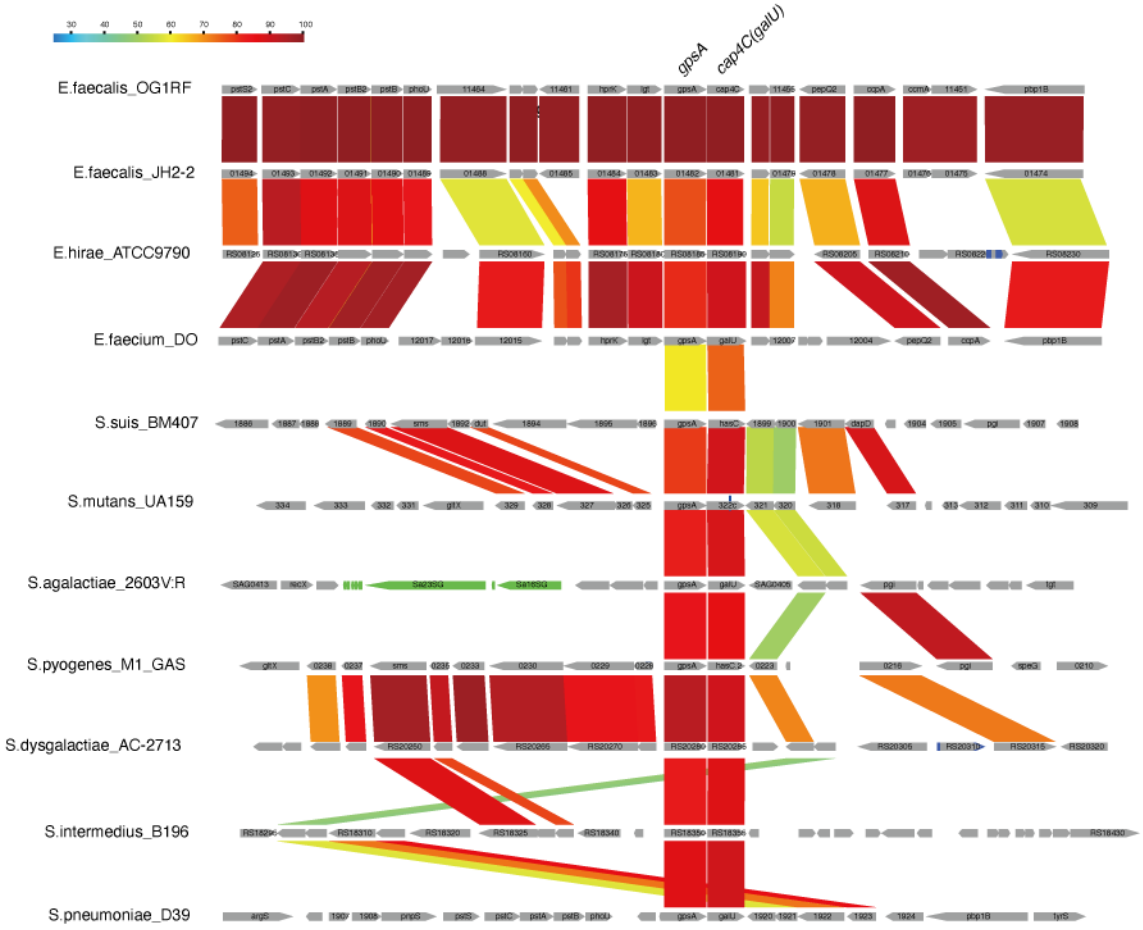

Supplementary figure S7. Genetic structure alignment for the flanking regions of *gpsA-galU* locus conserved among the Gram-positive bacterial species. Color scale represents similarity (%) of CDS based on the blastp analysis. The sequence data obtained from NCBI database (https://www.ncbi.nlm.nih.gov/). This scheme was generated using the GenomeMatcher software (http://www.ige.tohoku.ac.jp/joho/gmProject/gmhome.html) (1).

Fig. S8

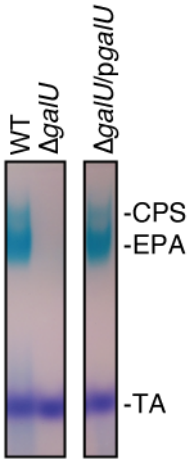

Supplementary figure S8. Effect of *galU* deletion on the cell wall-asociated polysaccharide production in *E. faecalis* FA2-2. The *E. faecalis* FA 2-2 wild type, Δ*galU*, and Δ*galU*/p*galU* strains were grown in THB broth supplemented with glucose, and the cell wall-associated polysaccharides were prepared as described in the Materials and Methods section. The resulting polysaccharides were separated via 10% acrylamide gel electrophoresis, followed by staining with the Stains-All reagent. CPS, Capsule polysaccharide; EPA, Enterococcal polysaccharide antigen; TA, Teichoic acid.